RSRO Report: Faraday Rotation Synthesis with AIPS and Three Bit Sampler Polarization Performance

David H. Roberts

Department of Physics MS-057, Brandeis University, Waltham, MA 02454-0911

roberts@brandeis.edu

ABSTRACT

I report on two topics, (1) the use of AIPS software to do Faraday Rotation Measure Synthesis (FRS) with Jansky VLA data on the micro-quasar SS 433, and (2) a comparison of the polarization performance of the three-bit and eight-bit samplers. My conclusions are that (1) the AIPS FRS software seems to work well and is useful in uncovering features of SS 433, and (2) the polarization crosstalk of the three- and eight-bit systems are very similar but not identical.

Wednesday 12th December, 2012

Contents

List of Figures

1. INTRODUCTION

2. SS 433

The famous source SS 433 is a micro-quasar with two oppositely-directed precessing jets. A multi-frequency synthesis image of SS 433 in total intensity is shown in Figure 1; this was made with several rounds of self-calibration in CASA using the tasks CLEAN (terms = 2), GAINCAL, and APPLYCAL.

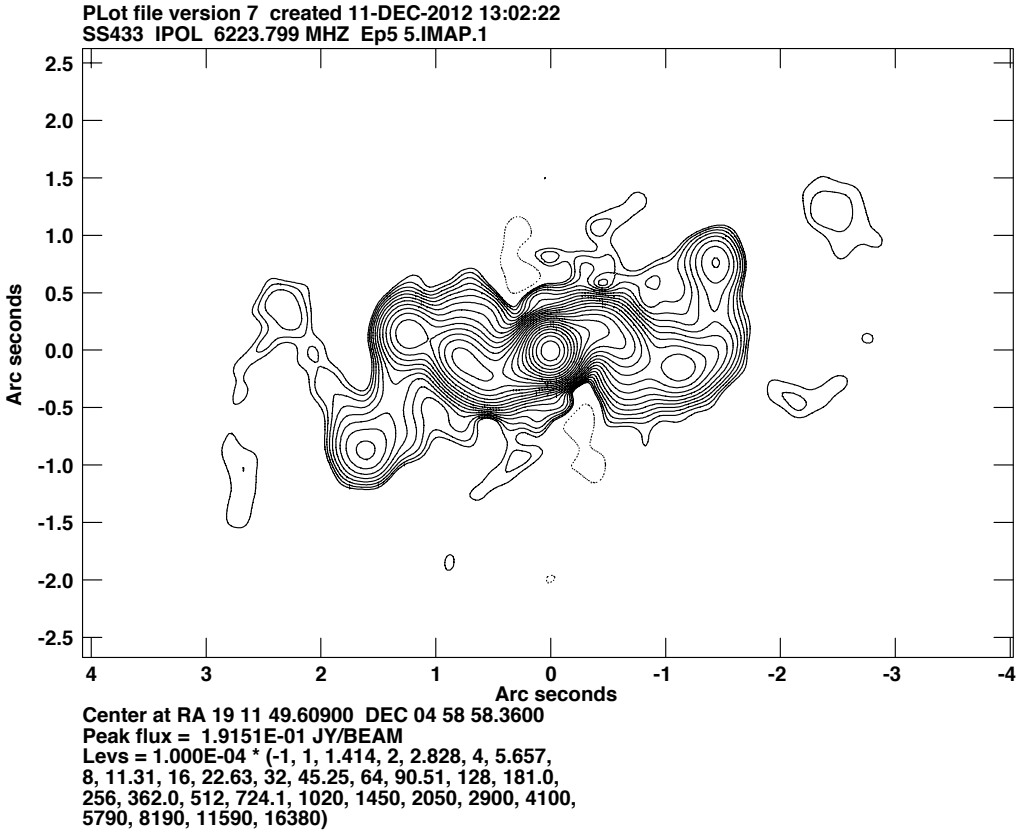

Fig. 1.— C band image of SS 433 made with the VLA in the A-array, epoch 2011 July 30.

3. FARADAY ROTATION MEASURE SYNTHESIS

Many radio sources contain significant Faraday rotation, produced either by a foreground screen or intrinsic to the source (or a combination of the two). For polarization-sensitive observations with a wide-band interferometer such as the Jansky Very Large Array, this can result in differential Faraday rotation across an observing band that will distort the polarization if it is measured by a conventional multi-frequency synthesis. The technique of FRS was developed to overcome this difficulty. In addition, in principle FRS can provide information about the three-dimensional structure of a source that cannot be obtained in any other way.

This technique is based on the work of Burn (MNRAS, 133, 67 (1966)), as applied to wide-band synthesis data by Brentjens and de Bruyn (A&A, 441, 1217 (2005)). The basic idea is that the contribution to the net linearly polarized radiation received by the observer from various layers of the source can be described by a Faraday dispersion function $F(\phi)$, where F is the contribution

made at Faraday depth ϕ, where

$$\phi = \int n_e B_\parallel \, dl.$$

The function F is the source function for the complex polarization $P = Q + iU$ formed from the Stokes parameters for linear polarization Q and U, according to

$$P(\lambda^2) = \int_{-\infty}^{+\infty} F(\phi) e^{2i\phi\lambda^2} \, d\phi.$$

Since this is a Fourier-like relation, in principle with sufficient coverage of λ^2-space and a suitable deconvolution algorithm like CLEAN it can be inverted to recover $F(\phi)$; this is what a FRS code is designed to do. In AIPS it is implemented in the tasks FARS, AFARS, and RFARS; useful tasks for visualization of the results include PLCUB, ISPEC, and KNTR.

3.1. FARS

This task performs the Fourier inversion and CLEAN in Faraday depth space to produce spectral line-like cubes containing the real and imaginary parts of $F(\phi)$ for a range of ϕ specified by the user. (If asked it will output amplitude and phase instead of real and imaginary parts.) It is often convenient to use the procedure DOFARS to implement FARS. The input data are cubes of Q and U images of the source made by standard imaging software in suitably narrow spectral windows that bandwidth depolarization is not a problem. In my tests these images were made in CASA and moved to AIPS where the cubes were assembled by the task FQUBE. The input u-v data were 32 128-MHz wide spectral windows in the ranges 4488–5512 and 6938–7066 MHz (C-band). The data were calibrated in CASA and individual Q and U images were made one spectral window at a time. FARS was run with default parameters, which for this frequency range resulted in a Faraday depth resolution of about 1031 rad m^{-2} and cells of 271 rad m^{-2}; we used a total of 51 cells (APARM(1) = 25).

To visualize all the information in the cubes output by FARS one can use the tasks PLCUB, ISPEC, and KNTR. Figure 2, produced by PLCUB, shows the Faraday spectrum every one-half beam width across SS 433. What is displayed there is the logarithm$_{10}$ of the magnitude of F in Jy/beam as a function of Faraday depth (only the central part of ϕ-space is shown).

Another useful way to visualize the output of a FRS is to make contour images of the intensity of F at various Faraday depths. In addition, the phase of F can be plotted on a color scale on top of these contours. This is accomplished with the AIPS task KNTR; see Figure 3. There is clearly a great deal of information about the structure and magnetic fields in SS 433 in these images, but we have not yet had time to analyze them.

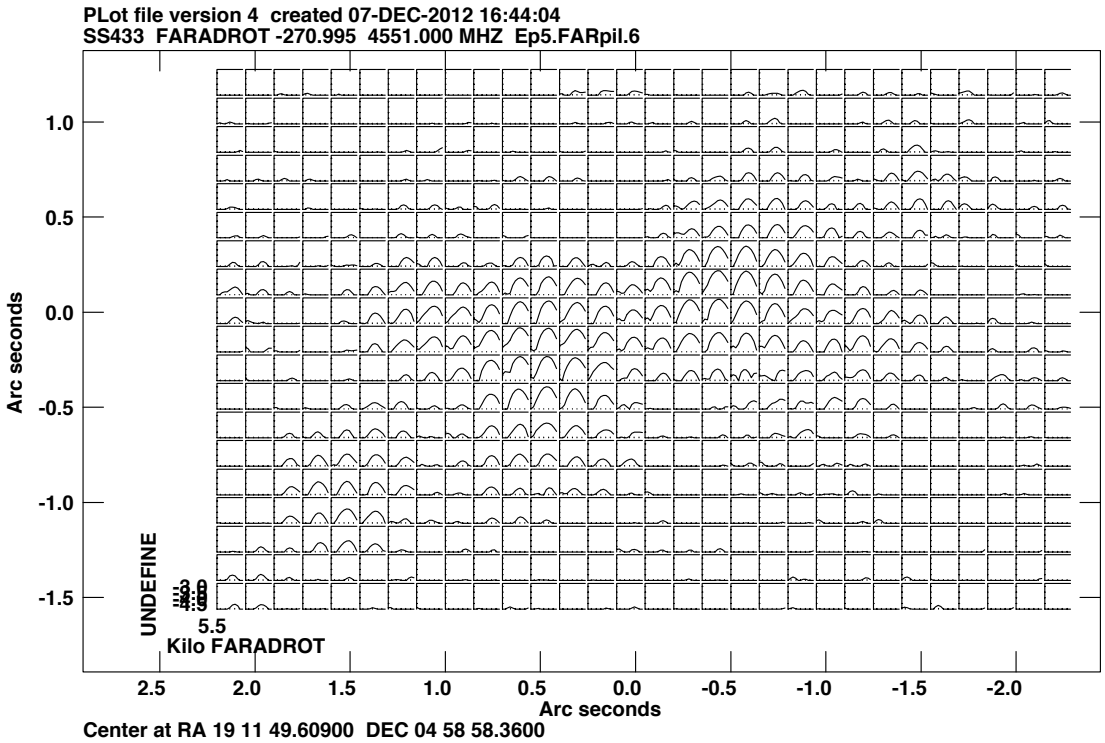

Fig. 2.— Faraday spectra of SS 433 at positions across the source spaced by one-half beam width in each direction. The abscissae are the Faraday depth and the ordinates the $\log_{10}$ of the magnitude of F. Compare to Figure 1.

3.2. AFARS

This task searches the output of a FARS image cube image-pixel-by-image-pixel, and for each finds the Faraday depth at which the magnitude of F is greatest. It then reports that Faraday depth, as well as the amplitude and phase of F there. This output is in the form of 2-D images and may be plotted with standard AIPS tasks such as CNTR and PCNTR. An example of the distribution on the sky of Faraday depth at the maximum of F is shown in Figure 4. We compared such images to rotation measure images made by the task FARAD and found the agreement to be generally very good.

3.3. RFARS

This task uses the output of AFARS to correct the input Q and U cubes for Faraday rotation. The various planes of the resulting cubes can be summed with the task SQASH to form Q and U images that have had the differential Faraday rotation removed. Such a polarization intensity image is used in Figure 4.

3.4. Conclusions I

All our tests suggest strongly that the AIPS FRS code works as advertised. We believe it will be very useful, even essential, for doing polarimetry with the VLA in the future.

Further we suggest that FRS code be incorporated into CASA, possibly based on the three-dimensional deconvolution algorithm of Bell & Ensslin (A&A, 540, 80 (2012)) and its extension with maximum entropy estimation (Bell, Oppermann, Crai, & Ensslin, astro-ph:1211.5105).

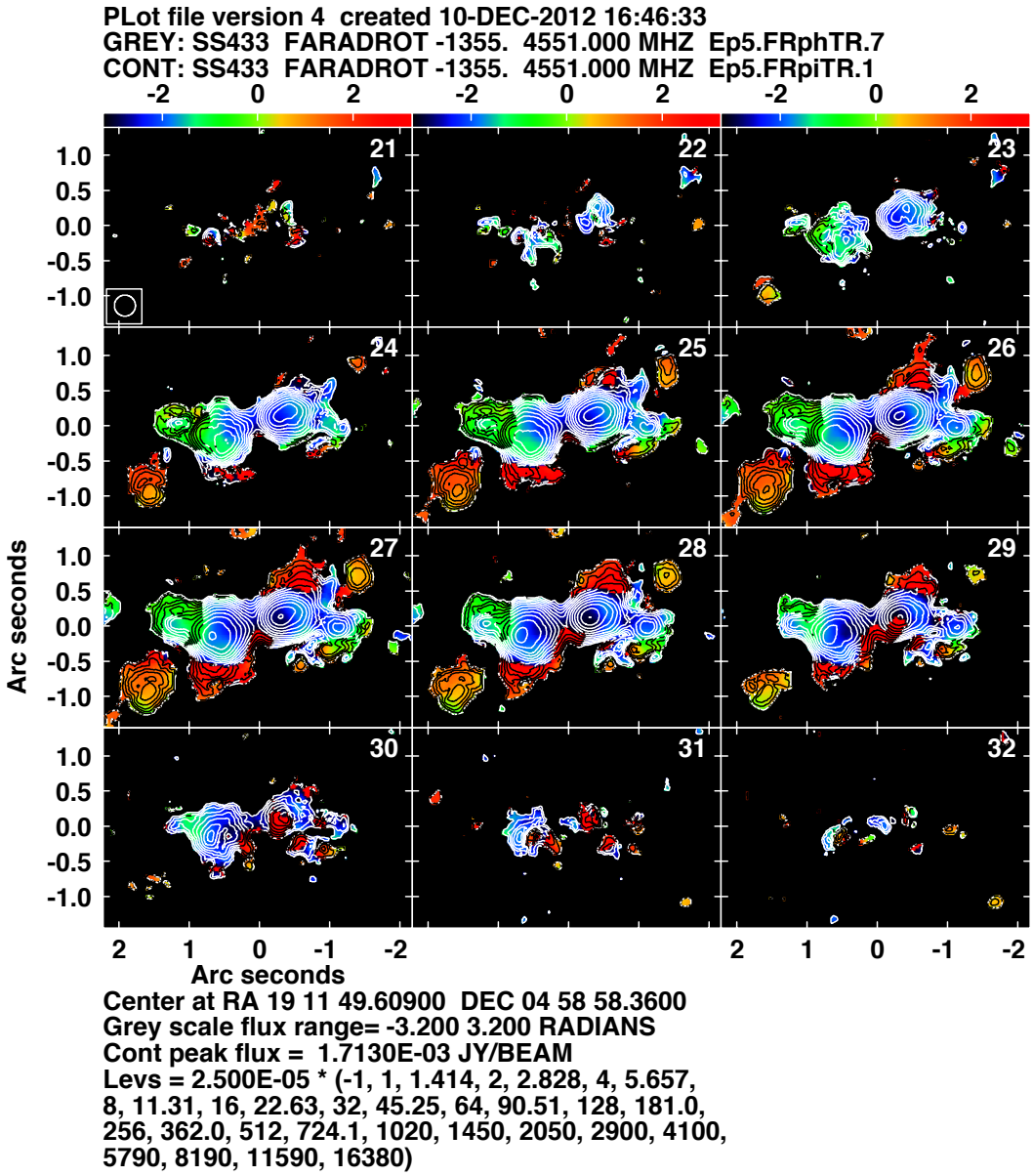

Fig. 3.— "Channel maps" of SS 433 at a series of Faraday depths ϕ. Channel 26 is $\phi = 0$, and the steps are 271 rad m^{-2} per channel increasing with channel number. The contours are the amplitude of $F(\phi)$ and the colors its phase (radians) on the scales on top.

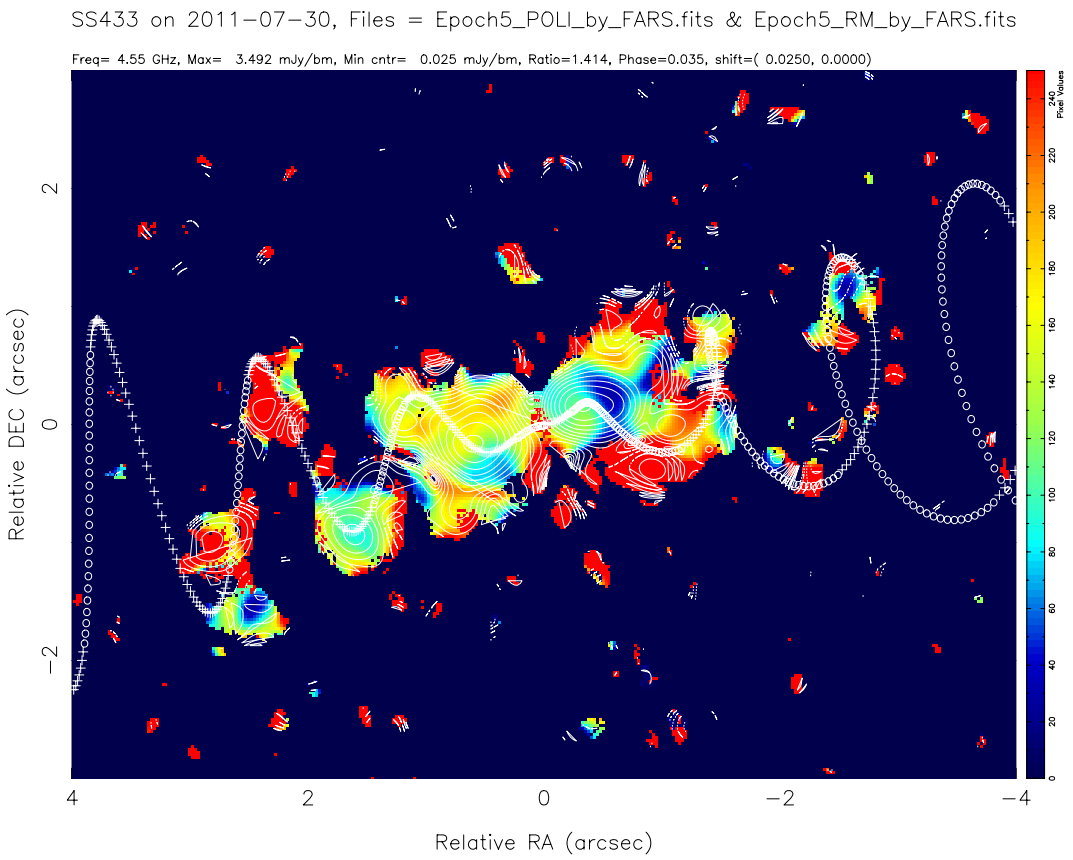

Fig. 4.— Faraday rotation in color on the scale to the right over contours of polarized intensity of SS 433. The helices are the optical model. This plot was produced by Brandeis software.

4. TESTS OF THE POLARIZATION PERFORMANCE OF THE THREE-BIT SAMPLER SYSTEM

4.1. Introduction

An essential part of the polarization response of the VLA is characterized by the polarization cross-talk, the response of a receiver system designed for one polarization to the orthogonal polarization. This is parameterized by the D-terms. The purpose of the exercise was to compare the D-terms present in the eight-bit system to those in the three-bit system by observation of a suitable polarization calibration source.

4.2. The Data and Calibration

We studied the frequency structure of the D-terms with data taken simultaneously with the eight-bit and three-bit systems (epoch 2012 October 24). The same frequencies on the sky (centered at 22.000 GHz) were observed in eight-bit mode (spws 0–7) and in two separate three-bit setups (spws 12–19 and 28–35). A single source, 3C 84, was used. The data were calibrated in CASA, the steps being (1) editing out bad antennas, (2) flagging the edges of the spw's, (3) finding the delays, (4) doing a bandpass calibration, (5) finding a gain solution, (6) determining the D-terms, and (7) applying all of the resulting calibration tables. As there were no other calibrators in the data it was not possible to determine the polarized delays. In addition, the flux of 3C 84 was set at 30 Jy which is about what previous observations showed at this epoch. We assumed that 3C 84 was unpolarized because we had no choice given the limited time span of the data; it is known that there is some small linear polarization in this source in K-band, which is a potential source of very small errors in the results.

4.3. Results

A small subset (LCP, six antennas) of the D-terms found for each of the three data paths are shown in Figures 5–7.

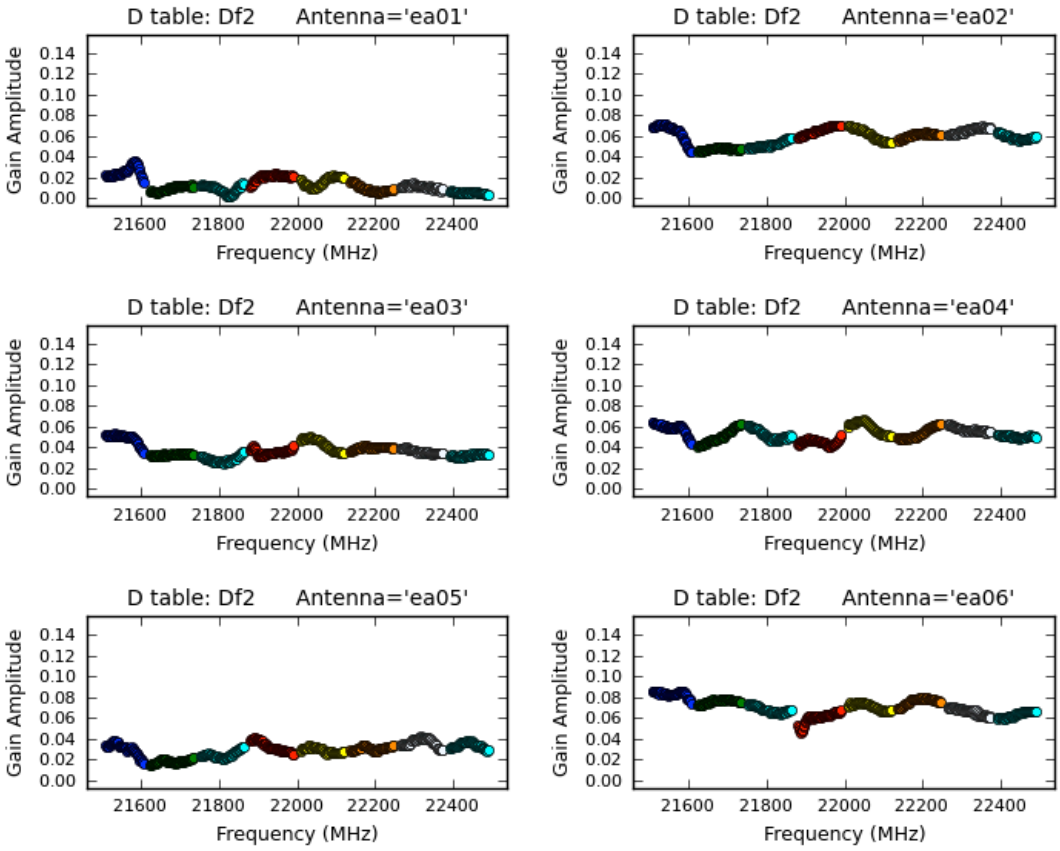

Fig. 5.— Some D-terms for the eight-bit system (spw's 0–7).

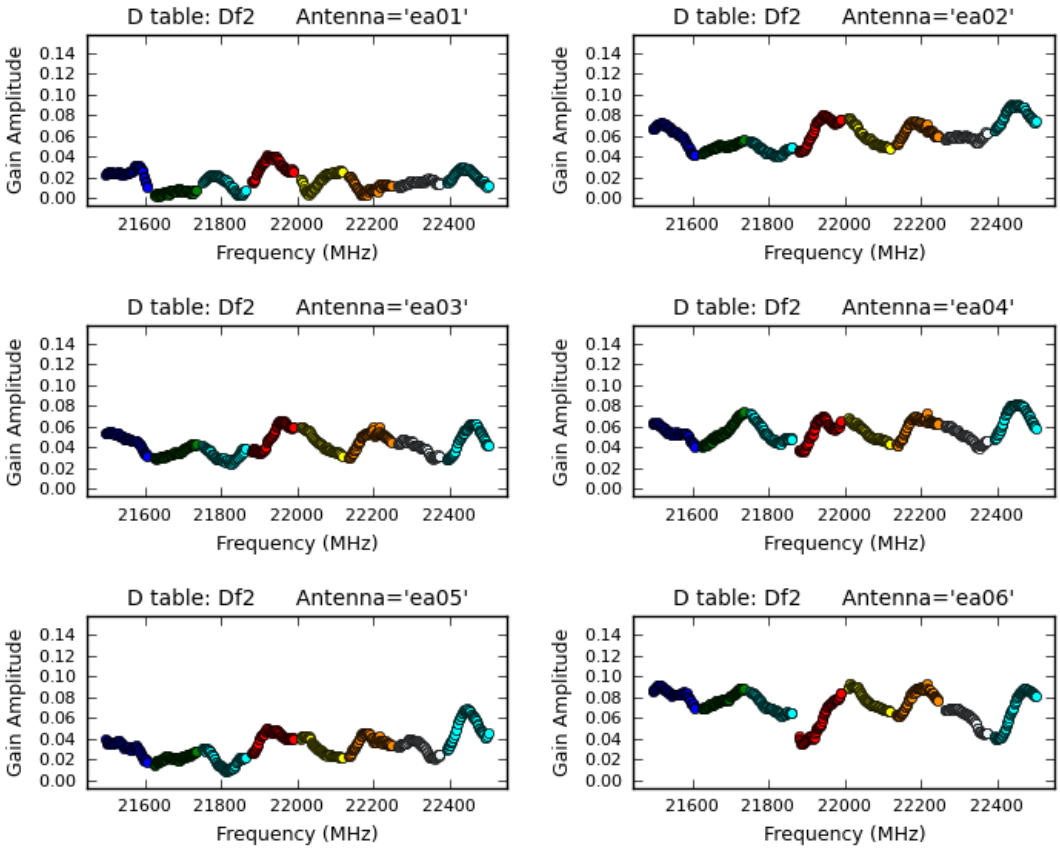

Fig. 6.— Some D-terms for the three-bit system (spw's 12–19).

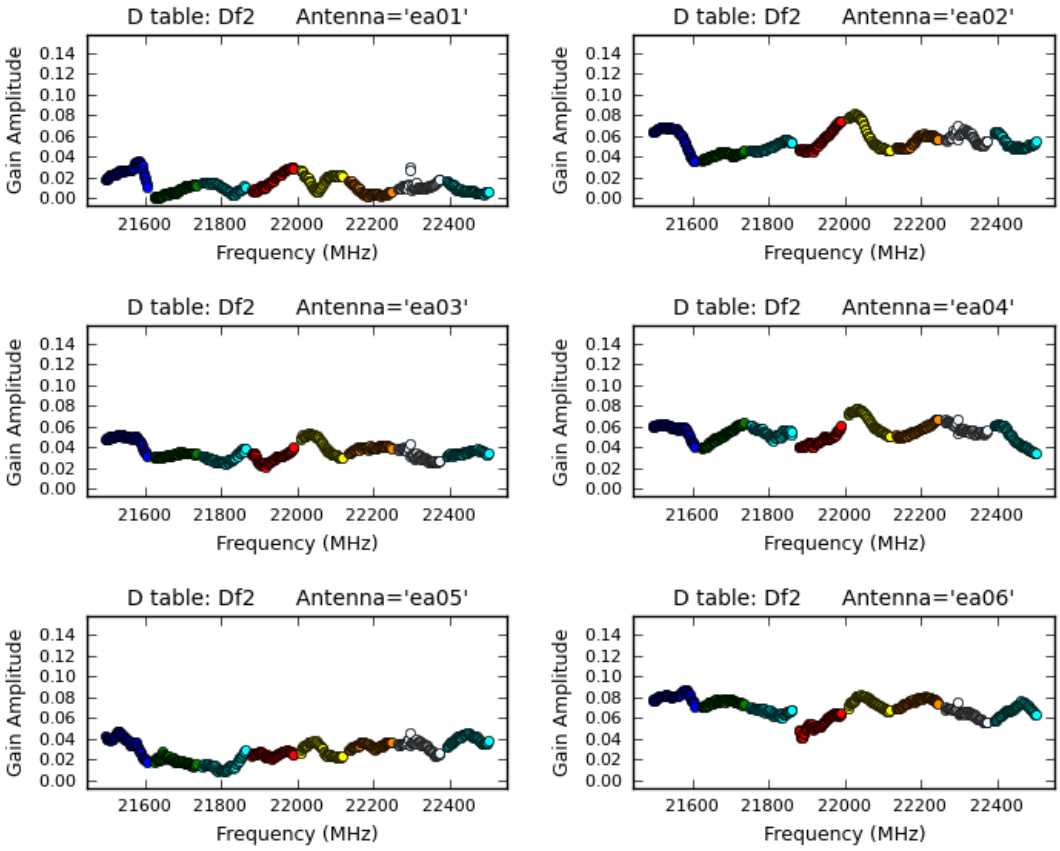

Fig. 7.— Some more D-terms for the three-bit system (spw's 28–35).

Comparison of the D-terms in the two systems shows that they are very similar in amplitude and overall frequency structure antenna-by-antenna. However, there do appear to be ripples in the structure of the three-bit D-terms that are not present in the eight-bit system. These appear to be at the 1–2% level out of typical amplitudes of 5%. The two three-bit systems each contain the ripples, and they are similar but not identical.

4.4. Images of 3C 84

After determining the D-terms we made total intensity and polarization images of 3C 84 using CLEAN (nterms = 1). The I images for the eight-bit and one three-bit system are shown in Figures 8 & 9, with POLI images shown in Figures 10 & 11.

It seems that the polarization calibration was excellent in both the eight- and three-bit systems, as essentially no polarized flux shows up at the phase center in either case; deeper plots show that the POLI there is less than about 0.2 mJy/beam, which represents less than one part in 100,000 of the total intensity.

4.5. Conclusions II

Overall the polarization performance of the three-bit system seems comparable to that of the eight-bit system. There are apparently some small ripples in the frequency structure of the D-terms that are present in the three-bit system but not in the eight-bit system. If these ripples are real and stable in time, then they can be calibrated out and will make no difference to the results of a polarization-sensitive science observation.

A more comprehensive POLCAL run is being scheduled to study the end-to-end polarization performance of the three-bit system.

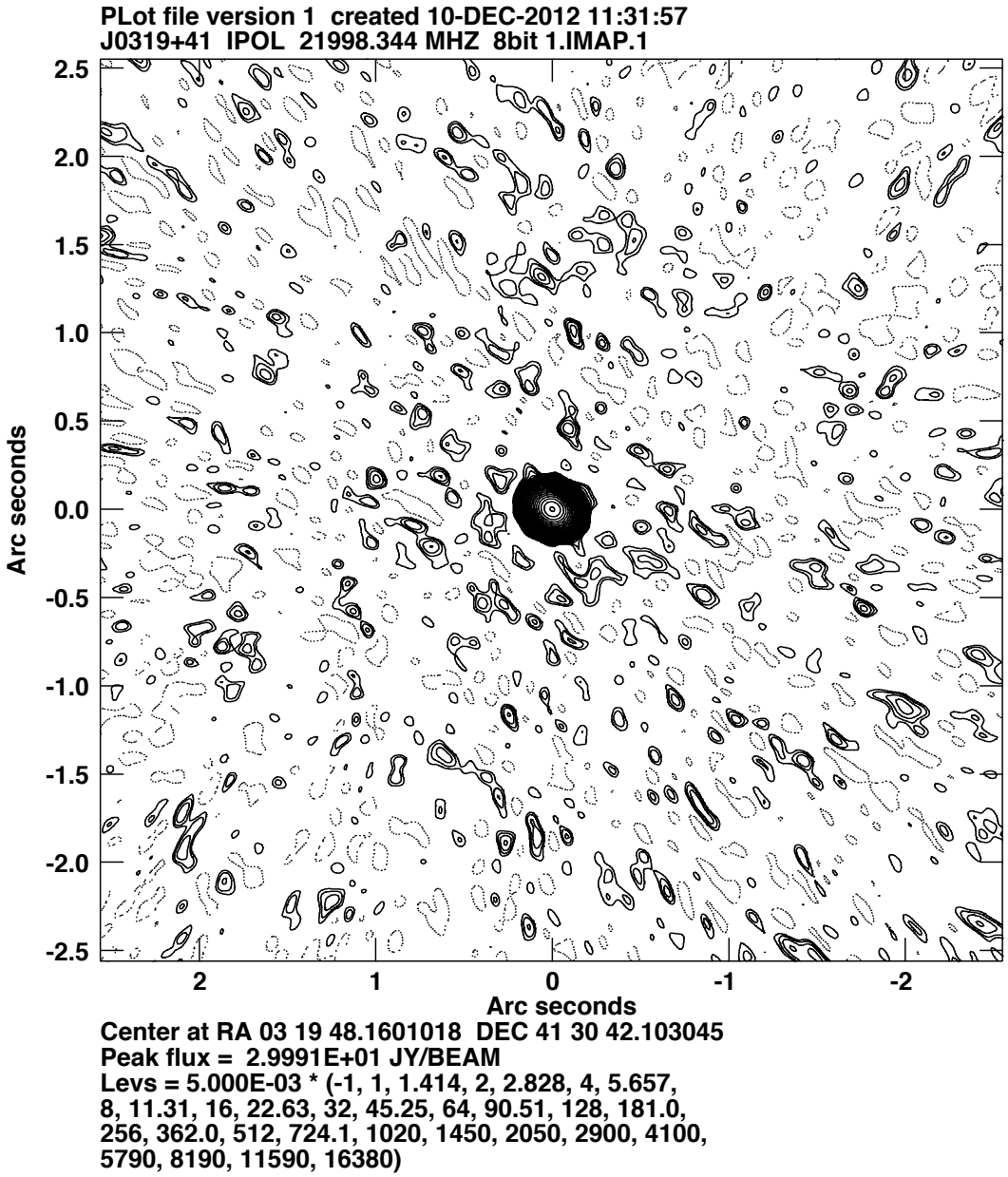

Fig. 8.— Total intensity image of 3C 84 made with the eight-bit system.

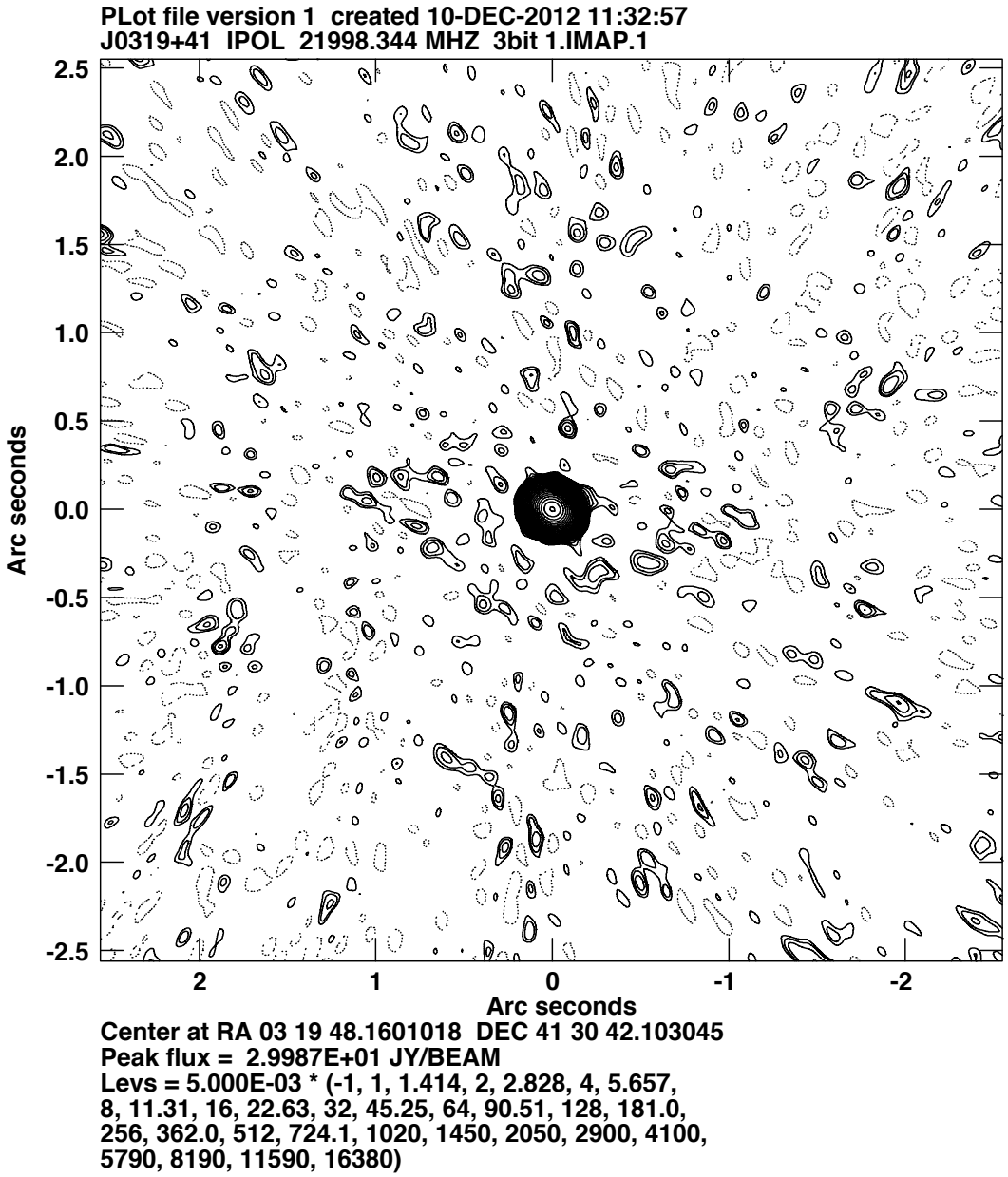

Fig. 9.— Total intensity image of 3C 84 made with the three-bit system.

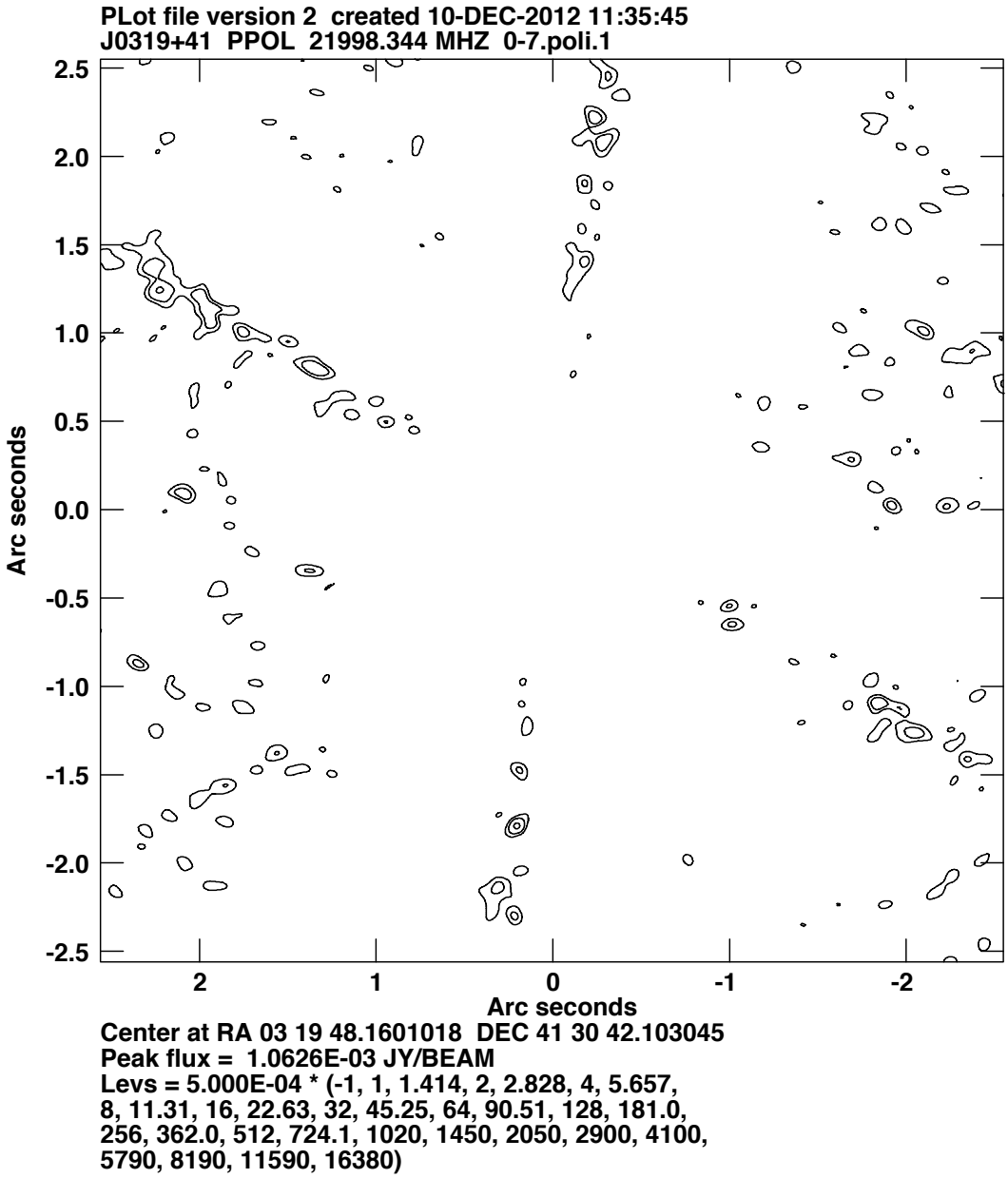

Fig. 10.— Polarized intensity image of 3C 84 made with the eight-bit system.

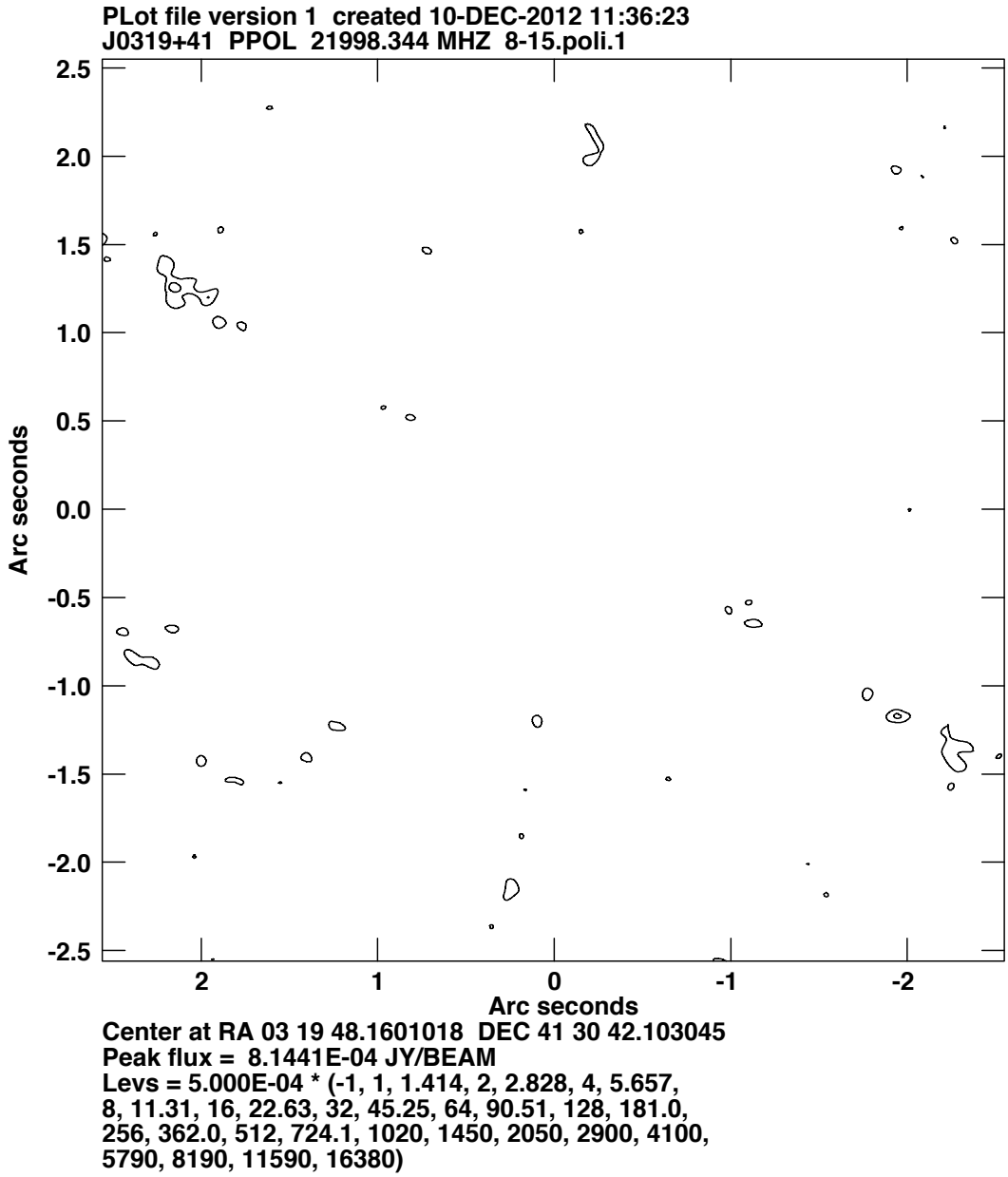

Fig. 11.— Polarized intensity image of 3C 84 made with the three-bit system.